ACS Photonics

Letter

pubs.acs.org/journal/apchd5

Resolving Light Handedness with an on-Chip Silicon Microdisk

Francisco J. Rodríguez-Fortuño, Isaac Barber-Sanz, Daniel Puerto, Amadeu Griol, and Alejandro Martínez*

Nanophotonics Technology Center, Universitat Politècnica de València, Valencia, Spain

Supporting Information

ABSTRACT: The efficient manipulation of circularly polarized light with the proper handedness is key in many photonic applications. Chiral structures are capable of distinguishing photon handedness, but while photons with the right polarization are captured, those of opposite handedness are rejected. In this work, we demonstrate a planar photonic nanostructure with no chirality consisting of a silicon microdisk coupled to two waveguides. The device distinguishes the handedness of an incoming circularly polarized light beam by driving photons with opposite spins toward different waveguides. Experimental results are in close agreement with numerical results, which predict extinction ratios over 18 dB in a 20 nm bandwidth. Owing to reciprocity, the device can also emit right or left circular polarization depending on the chosen feeding waveguide. Although implemented here on a CMOS-compatible platform working at telecom wavelengths, the fundamental approach is general and can be extended to any frequency regime and technological platform.

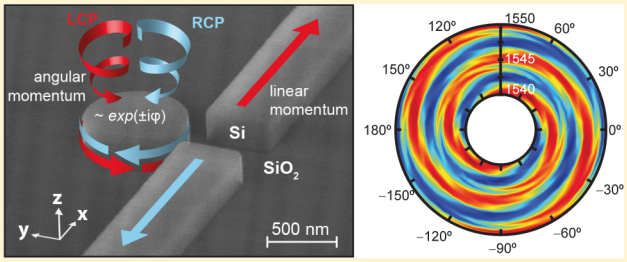

KEYWORDS: *nanoantenna, polarization, silicon, spin, spin−orbit, angular, momentum, coupling*

Individual photons have left- or right-handed circular polarization. From a quantum perspective, it can be said that each photon carries an intrinsic spin angular momentum (SAM), which takes the value of $+\hbar$ for left-handed circular polarization (LCP) and $-\hbar$ for right-handed circular polarization (RCP). Circularly polarized light (CPL) is used in a wide variety of applications, such as ellipsometry,[1] astronomy,[2] magnetic recording,[3] cooling,[4] quantum polarization encoded qu-bits,[5] and molecular spinning measurements.[6] Therefore, the availability of photonic structures that enable the manipulation of CPL is extremely interesting. However, the determination of the sign of the handedness of a CPL beam in a miniaturized setup is not straightforward.[7,8] Typically, chiral structures, in which the chirality can be defined either at a molecular level[8] or by micro- or nanostructuring,[9−12] respond differently to the two circular polarizations; for example, one is accepted, while the orthogonal one gets reflected. More sophisticated 3D structures[7] can split up LCP and RCP, directing them to different directions, but with extinction ratios below 5. In order to avoid complex 3D nanostructuring, it would be highly desirable to implement such a functionality on a planar substrate, which has been recently demonstrated by using apertures on thin metal planes displaying chiral-like responses.[13] However, such plasmonic structures achieve experimental extinction ratios of CPL below 2 and require nanometric resolution, which can be achieved by fabrication tools such as focused ion beam, not suitable for large-scale production. Moreover, even when implemented on a planar substrate, the response continues being chiral and thus selects one handedness while rejecting the other one, so the enantiomeric structure is required to detect the opposite handedness. Nonchiral plasmonic structures capable of sorting both RCP and LCP equally into mirror-symmetric propagation directions in the same structure have been demonstrated, relying on breaking the mirror symmetry in the orthogonal direction;[14−17] however this approach has been so far limited to plasmonics, in technological platforms not readily suitable for mass production.

Here, we describe a novel approach to detect the SAM, or handedness, of CPL, which is fully implemented on a CMOS-compatible silicon photonics platform. We show theoretically and experimentally that the fundamental resonance of a silicon microdisk resonator can inherit the angular momentum carried by a normally incident light beam and transfer it as linear momentum into one of two output waveguides. The microdisk is not chiral: it responds equally to LCP and RCP without exhibiting optical activity nor circular dichroism. Instead, it couples light to different waveguides (with opposite linear momenta) depending on the handedness of incoming light and the relative position between the microdisk and the waveguides. Moreover, reciprocity inspired us to demonstrate that in transmission the microdisk behaves as a dielectric nanoantenna that emits circularly polarized light with a handedness determined by the feeding waveguide. Since our approach is based on the coupling between a circular resonator, supporting modes with angular momentum, and a waveguide, it is very general and can be translated to other photonic integrated circuit (PIC) platforms as well as to other frequency regimes.

Received: March 20, 2014
Published: August 26, 2014

Our photonic structure could find direct applications in integrated ellipsometry and quantum processing.[5]

RESULTS AND DISCUSSION

Description of the Approach. Our approach is based on a circular microdisk resonator, known to support resonant whispering gallery modes displaying angular momenta given by $\pm l\hbar$, where l is the azimuthal number.[18] Typically, such modes display ultrahigh Q factors and, therefore, do not radiate to free space unless properly tailored scattering elements are inserted.[19] However, the situation is different for small-size resonators (in terms of wavelength). In that case, the fundamental mode $l = 1$, which is essentially a highly radiative dipolar resonance, is the dominant scattering contribution.[20] Under normal incidence with CPL, one of the two degenerate fundamental modes, with an angular momentum per photon equal to $+\hbar$ (for LCP) or $-\hbar$ (for RCP), is excited. In other words, there is an angular momentum transfer and match between the incoming CPL light beam and the microdisk resonator. The mode can also be seen as the superposition of two 90° phase-shifted linearly polarized Mie dipolar resonances in the microdisk. Due to its radiative nature, the $l = 1$ resonance is very broad in frequency, so there is no need to work exactly at the center of the resonance. Instead, as long as the dipole-like mode is excited, the device can be operated in a broadband region. Part of the spin angular momentum of the incoming light beam is coupled into orbital angular momentum in the microdisk whispering gallery resonance, so this mechanism is an example of spin−orbit coupling.

Now let us consider that the microdisk resonator is implemented on a PIC platform close to a waveguide. Figure 1 is an annotated scanning electron microscope (SEM) image of the fabricated structure showing the fundamental idea. It is well known that the resonant modes of a microdisk can be excited on-chip by introducing light through an optical waveguide, which at some point is in close proximity to the microdisk,[18] and the direction of propagation of light along the waveguide (or the direction of the linear momentum of the guided photons) will define the direction of rotation of the fields inside the microdisk at the resonance frequencies, due to local phase matching in the interacting region, and, as a consequence, will define the sign of the excited angular momentum. In accordance to reciprocity, the reverse approach is also true: if a given resonance in the microdisk is excited from free space using CPL, part of the angular momentum transferred to the microdisk will be finally converted into linear momentum, which will result in light propagation along one or another direction of the waveguide depending on the handedness of incident light. An alternative interpretation, which inspired us to pursue this result, is that the microdisk simply acts as a polarizable particle that gets circularly polarized from incident CP light and results in unidirectional excitation of guided modes due to near-field interference.[14] Therefore, the device will be capable of discerning between LCP and RCP without employing chiral structures. Notice that the placement of the microdisk with respect to the waveguide will determine the sorting direction of each handedness. The x-asymmetry achieved in the amplitude of excitation of the two waveguide outputs is possible only due to the broken y-symmetry in the whole (microdisk + waveguide) structure, which constitutes a fundamental requirement of this approach. Otherwise, in a y-mirror symmetric structure, only the vertically polarized component of incident plane waves can couple to either

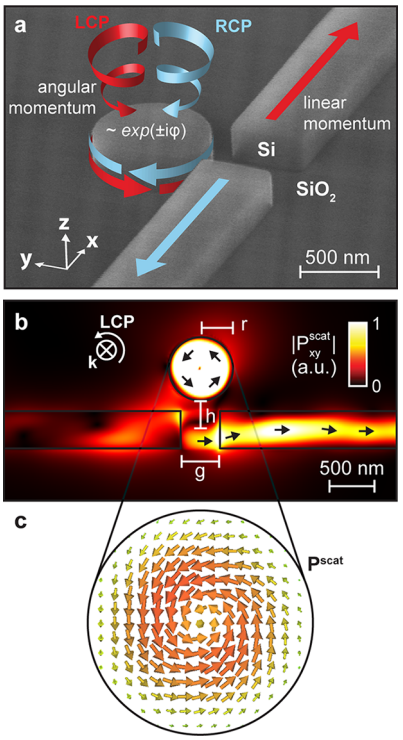

Figure 1. Concept and simulation. (a) Scanning electron microscope (SEM) image of the fabricated microdisk and silicon waveguide, annotated with arrows describing the fundamental idea of this approach. (b) Magnitude of the in-plane component of the Poynting vector of the scattered fields in the midplane of the silicon structure when a LCP plane wave is incident. (c) Vector plot of the Poynting vector of the scattered fields in the midplane inside the nanodisk.

waveguide, and both circular polarizations are excited with equal amplitudes to either side. For this reason we use such a symmetric structure as a control in our experiments. A formal discussion about the symmetry is given in the Supporting Information.

Numerical Results. We numerically modeled a normally incident plane wave onto the silicon microdisk placed near a standard 250 × 400 nm single mode silicon waveguide in a silica substrate and studied the amplitude of the waveguide TE-like mode excitation toward either side as a function of the incident polarization. The performance can be measured through the extinction ratio, defined as the ratio between intensities excited toward the desired and undesired outputs under normally incident pure CPL illumination. This is also the ratio of the LCP and RCP excitation toward the same given output, as discussed in a formal model of the system in the Supporting Information. To optimize the extinction ratio and increase the coupling between the microdisk and the waveguide, we tuned the radius r of the microdisk and its distance to the center of the waveguide h, and, importantly, we introduced an air gap g in the waveguide, which increases the amount of coupled light while leaving the physical mechanism essentially unchanged. The dependence of the figure of merit and coupling efficiencies on the gap length is included in Supporting Information Figure S3, showing that the presence of the gap strongly enhances the coupling efficiency. We maximized the extinction ratio at 1550 nm while trying to keep a reasonable effective area. After optimization, a radius r = 340 nm, separation of h = 300 nm, and waveguide gap of g = 400 nm resulted in an extinction ratio between outputs for CPL

dx.doi.org/10.1021/ph500084b | ACS Photonics 2014, 1, 762−767

greater than 18 dB in the wavelengths of 1540 to 1560 nm, reaching up to 30 dB at 1550 nm, while the effective area of the device (defined as the power coupled into the TE-like mode of the waveguide over the incident plane wave power density) is around 0.05 μm^2 at 1550 nm (13% of the area of the microdisk and ranges between 10% and 18% throughout the 1540 to 1560 nm wavelength range). Supporting Information Figure S2 shows the graph of the calculated effective area for each waveguide output under CPL illumination. Although only a small fraction of the incident light is ultimately captured into either waveguide, the fraction of optical intensities detected at either side corresponds to the handedness components of incident light with great accuracy. Figure 1b shows the absolute value of the in-plane Poynting vector component of the scattered fields in the middle plane of the structure at 1550 nm under LCP illumination, together with a vector visualization of the full Poynting vector inside the microdisk (Figure 1c), clearly indicating that the mode $l = 1$, with an optical angular momentum, is excited in the microdisk. Numerical studies of the microdisk, included in the Supporting Information, reveal that the $l = 1$ mode of our microdisk is centered at around 1600 nm, but a low Q factor of 4.2 allows its excitation around 1550 nm with broadband operation, without working at the center frequency. Excitation of linear momentum in one direction of the waveguide is observed. An animated video of the z-component of the scattered magnetic field is included as a Supporting Information video, where the rotation of the fields inside the microdisk is clearly observed, together with the unidirectional excitation of the waveguide toward the right output. The opposite waveguide direction shows some excitation of higher order evanescent modes. Evidently, from symmetry, incident RCP light is directed into the opposite waveguide output. Resolving the handedness of incident CPL can thus be achieved by a simple measurement of the two waveguide output intensities. Electromagnetic reciprocity implies that the microdisk, working as an emitter being fed from one of the two input waveguides, will ideally emit purely CPL in the normal direction. Formally, as shown in the Supporting Information, from simulations we can readily calculate that an elliptical polarization [eccentricity of 0.35 at a wavelength of 1550 nm, very close to circular] is emitted.

Experimental Results. We experimentally tested the device for both sorting and synthesis of CPL. Since the generation and detection of linearly polarized light at telecom wavelengths is easier and more experimentally robust than that of CPL, our experiments were designed to allow us to infer the properties of CPL indirectly through linearly polarized light measurements, as explained below.

In a first experiment, a lensed fiber was used to illuminate the microdisk with linearly polarized light, coming from a laser tuned at 1550 nm, exciting the microdisk. Light was then coupled from the microdisk to the silicon waveguide, which was cut at the edge of the sample, as shown in Figure 2a. As a control experiment, a waveguide with two microdisks symmetrically placed at either side (which responds only to y-polarized incident electric fields due to symmetry considerations described in the Supporting Information) was illuminated and measured simultaneously with the main experiment. The intensity of both spots was measured (see details in Methods) and plotted as a function of the illuminating linear polarization angle. The result is depicted in Figure 2b. The control structure, which responds only to y-polarized fields, clearly displays a strong $\sin^2(\theta)$ dependency of

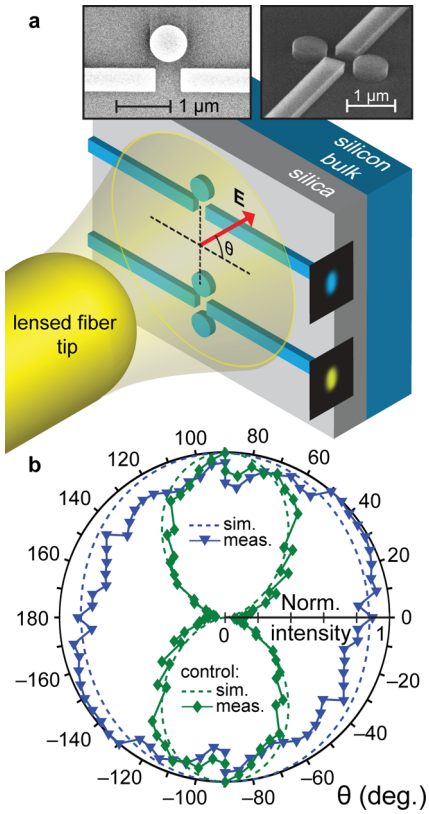

Figure 2. Reception experiment. (a) Schematic depiction (not to scale) of the experiment for reception of polarized light. SEM images of the fabricated designed and control structures are provided in the insets. (b) Experimentally measured intensity of the two output waveguide spots as a function of the polarization of incident radiation from the fiber tip, together with the corresponding simulations.

the spot intensity with the incident polarization angle. However, for the optimized single-microdisk structure, any linear polarization, being an equal superposition of RCP and LCP, will excite both output waveguide directions equally, so a spot intensity approximately independent of the incident linear polarization angle is observed at the waveguide output. This is an indirect proof that the device indeed resolves the handedness of incoming CPL directing each handedness into a different waveguide, as shown in detail in the Supporting Information following symmetry considerations.

In a second experiment we demonstrate the emission of polarized light by the microdisk. The fabricated setup is depicted in the SEM image of Figure 3a. The microdisk was fed from the two waveguides simultaneously with equal amplitudes but different phases, by using a symmetric Y-splitter followed by two optical paths with a length difference of ΔL. The phase difference between both inputs was $\Delta\varphi = 2\pi n_{eff}\Delta L/\lambda_0$, where λ_0 is the wavelength and $n_{eff} = n_{eff}(\lambda_0)$ is the effective index of the waveguide mode. Ideally, light incoming from each input radiates CPL of opposite handedness, and the superposition of the radiated LCP and RCP light with different relative phases leads to the synthesis of linearly polarized light, polarized at an angle determined by $\Delta\varphi$. Thus, emitted light that is linearly polarized at an angle inversely proportional to the wavelength is expected. The radiated intensity from the microdisk at different wavelengths from 1540 to 1550 nm measured in steps of 0.5 nm was plotted as a function of the angle of a free-space linear polarizer placed before the microscope. The resulting 2D plot is

dx.doi.org/10.1021/ph500084b | ACS Photonics 2014, 1, 762−767

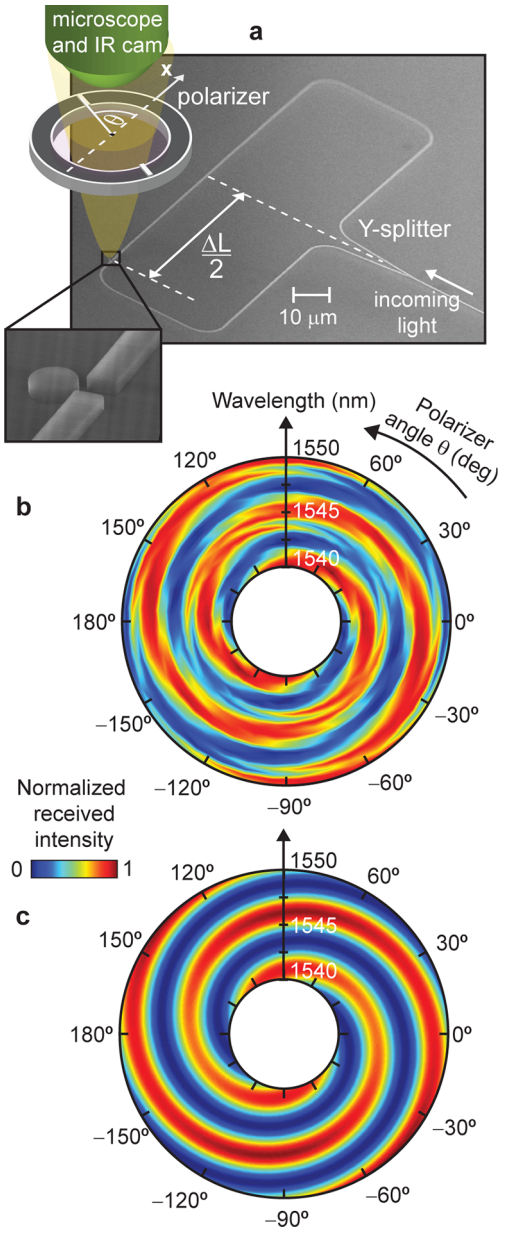

Figure 3. Emission experiment. (a) Annotated SEM image of the fabricated silicon photonic circuit used to generate linearly polarized light from the superposition of LCP and RCP and schematic of the detection scheme. $\Delta L/2 = 50\ \mu$m. (b) Experimentally measured radiated intensity by the microdisk as a function of the polarizer rotation. (c) Corresponding numerical simulation.

shown in Figure 3b. The spiral corresponds to the synthesis of linear polarizations whose electric field orientation varies with the wavelength. The optical path length difference of $\Delta L = 100\ \mu$m ensures that all possible relative phases between both inputs are achieved. The corresponding simulations are shown in Figure 3c, exhibiting the general spiral pattern observed in the experiment. Quantitatively, the measured ratio from maximum to minimum intensity received at each wavelength determines how close the emitted light is to a linear polarization. Simulations show an extinction ratio of >18 dB in the whole range, while experimentally it is always >10 dB, except for the small region 1543.5−1544.5 nm, where it reaches only 5 dB (see Supporting Information Figure S5). This slight disagreement, together with the apparent "twisting" observed in the measurement and not present in the simulation, might arise from imperfect fabrication, unequal losses in the two paths, fabrication asymmetries in the Y-splitter, surface roughness in the microdisk potentially coupling the two counter-propagating microdisk modes, and Fabry−Perot-like multiple reflections in the waveguide bends, splitter, scatterer, and at waveguide imperfections, causing photonic interference in the circuit, all of which are not considered in the simulation. As detailed in the Supporting Information, by measuring the synthesis of linear polarizations when feeding the microdisk from both waveguides, this experiment indirectly proves that CPL would be emitted if the microdisk was fed separately from each input.

DISCUSSION

We have demonstrated the discrimination of LCP and RCP, in both a receiving and an emitting scheme, using a planar nonchiral structure implemented on a silicon photonics platform. We show that extinction ratios over 18 dB in simulations are achievable on a 10 nm bandwidth around the 1545 nm telecom wavelength. In experiments we measure extinction ratios greater than 11 dB from 1545 to 1549 nm, reaching 15 dB at some wavelengths, larger than those achieved using plasmonic nanostructures as reported in ref 13 or 3D chiral nanostructures,[7] with values lower than 7 dB for CPL. Our proposed device is not chiral nor does it contain chiral molecules, and it handles both LCP and RCP symmetrically and simultaneously with a single planar microdisk. Moreover, it does not exhibit optical activity (polarization conversion is not carried out) or circular dichroism. Instead, it is capable of handling each circular polarization equally and independently in both transmission and reception schemes. Numerical optimization is straightforward to implement, and fabrication follows well-known standard methods. This finding could be very useful for managing CPL in PIC platforms such as in silicon photonics, but since the concept is general, it can be translated to other technologies as well as to any band of the electromagnetic spectrum. The proposed photonic structure could be used in integrated ellipsometers, polarimeters, magnetic recording, cooling, molecular spinning, and other devices that require the generation and/or detection of CPL.

In our work, the angular momentum of the $l = 1$ whispering gallery resonance is coupled to and from freely propagating circularly polarized plane waves carrying the same angular momentum ($\pm\hbar$ per photon). The principle can be extended into higher orders, as described in ref 19, where high-order resonances in whispering gallery resonators with angular gratings are used for the generation of orbital angular momentum (vortex) beams, carrying an angular momentum higher than the $\pm\hbar$ per photon allowed in plane wave radiation. As an immediate application, the microdisk device presented here could be fabricated alongside the rectangular-shaped scatterer presented in ref 21, which allows the sorting of orthogonal linearly polarized light components. A complete characterization of the polarization of light incident into the structures would thus be possible in a fully integrated silicon photonics approach, since the six different polarization components of incoming light required to determine the Stokes parameters (RCP, LCP, and linear polarization in four different orientations) could be sorted into six different integrated waveguides whose intensity can be measured directly on chip. This is different from the plasmonic integrated polarimeter approach proposed in ref 13, where transmission measurements across six different structures are required.

dx.doi.org/10.1021/ph500084b | ACS Photonics 2014, 1, 762−767

METHODS

Numerical Simulations. Numerical simulations were performed with CST Microwave Studio. The silicon structures were modeled with a refractive index n = 3.45 and the silica substrate with n = 1.45. Geometrical symmetries were exploited as detailed in the Supporting Information. An incident plane wave pulse was simulated, with open boundary conditions in all directions, and the mode amplitude excited in the waveguide was recorded as a function of frequency. The mesh was improved locally until convergence of the results was obtained. The scattered fields plotted in Figure 1 were obtained by subtracting the background fields from the total fields. The background fields were obtained in a simulation of the same excitation but incident on a straight continuous waveguide (with no microdisk or gap).

Optical Experiments. The spot intensities at the output of the waveguides were measured with a Xenics Xeva 1508 IR camera mounted at the position of the eyepiece (in the absence of the eyepiece) of a 4× microscope (National Stereoscopic Microscopes Zoom model 420 series). This same setup was also used to measure the radiated intensity from the microdisk in the emission experiment, with the linear polarizer placed between the sample and the microscope.

To illuminate with linear polarizations in the reception experiment, we used a standard procedure in silicon photonics in which the orthogonal polarization at the output of the fiber is minimized. For this, the output fiber of a linearly polarized laser entered a fiber-polarization controller (FPC), which controls the polarization state of light at the output of the lensed fiber tip that illuminates the structures. The polarization of this illumination was monitored simultaneously to the reception experiment by using a free-space linear polarizer (extinction ratio >10.000:1 in the experimental range) and a Hamamatsu IR camera C2741 placed behind the substrate, transparent to IR radiation. To achieve a desired linear polarization at the output tip of the fiber, we use the FPC to minimize the orthogonal linear polarization at the output tip. The minimized orthogonal polarization reached power levels lower than −40 dBm (the detection limit of the camera), while the desired orthogonal polarization was always between −8 and −12 dBm.

Fabrication. The structures were fabricated on standard silicon-on-insulator (SOI) samples of SOITEC wafers with a top silicon layer thickness of 250 nm (resistivity ρ ∼1−10 Ω cm^{-1}, with a lightly p-doping of $\sim 10^{15}$ cm^{-3}) and a buried oxide layer thickness of 3 μm. The structure fabrication is based on an electron beam direct writing process performed on a coated 100 nm hydrogen silsesquioxane resist film. This electron beam exposure, performed with a Raith150 tool, was optimized in order to reach the required dimensions employing an acceleration voltage of 30 keV and an aperture size of 30 μm. After developing the HSQ resist using tetramethylammonium hydroxide as developer, the resist patterns were transferred into the SOI samples employing an also optimized inductively coupled plasma−reactive ion etching process with fluoride gases. Importantly, only a single lithography and etching step is needed to fabricate the structures, which stresses its simplicity.

ASSOCIATED CONTENT

Supporting Information

A formal mathematical model and description of the system, a study of the microdisk resonances, a discussion of the optimization and role of the air gap, a discussion of the y-symmetric control scatterer, and a mathematical justification of how the measurements involving linear polarizations are an indirect proof of the behavior under circular polarizations are all available free of charge via the Internet at http://pubs.acs.org.

AUTHOR INFORMATION

Corresponding Author

*E-mail: amartinez@ntc.upv.es.

Notes

The authors declare no competing financial interest.

ACKNOWLEDGMENTS

This work has received financial support from the Spanish government (contracts Consolider EMET CSD2008-00066 and TEC2011-28664-C02-02). D.P. acknowledges support from grant Juan de la Cierva (JCI-2010-07479).

REFERENCES

(1) Azzam, R. M. A.; Bashara, N. M. *Ellipsometry and Polarized Light*; North-Holland Pub. Co., 1977; p 529.
(2) Tinbergen, J. *Astronomical Polarimetry*; Cambridge University Press: Cambridge, 1996.
(3) Stanciu, C.; Hansteen, F.; Kimel, A.; Kirilyuk, A.; Tsukamoto, A.; Itoh, A.; Rasing, T. All-optical magnetic recording with circularly polarized light. *Phys. Rev. Lett.* **2007**, *99*, 047601.
(4) Arita, Y.; Mazilu, M.; Dholakia, K. Laser-induced rotation and cooling of a trapped microgyroscope in vacuum. *Nat. Commun.* **2013**, *4*, 2374.
(5) Crespi, A.; Ramponi, R.; Osellame, R.; Sansoni, L.; Bongioanni, I.; Sciarrino, F.; Vallone, G.; Mataloni, P. Integrated photonic quantum gates for polarization qubits. *Nat. Commun.* **2011**, *2*, 566.
(6) Korech, O.; Steinitz, U.; Gordon, R. J.; Averbukh, I. S.; Prior, Y. Observing molecular spinning via the rotational Doppler effect. *Nat. Photonics* **2013**, *7*, 711−714.
(7) Turner, M. D.; Saba, M.; Zhang, Q.; Cumming, B. P.; Schröder-Turk, G. E.; Gu, M. Miniature chiral beamsplitter based on gyroid photonic crystals. *Nat. Photonics* **2013**, *7*, 801−805.
(8) Yang, Y.; da Costa, R. C.; Fuchter, M. J.; Campbell, A. J. Circularly polarized light detection by a chiral organic semiconductor transistor. *Nat. Photonics* **2013**, *7*, 634−638.
(9) Gansel, J. K.; Thiel, M.; Rill, M. S.; Decker, M.; Bade, K.; Saile, V.; von Freymann, G.; Linden, S.; Wegener, M. Gold helix photonic metamaterial as broadband circular polarizer. *Science* **2009**, *325*, 1513−1515.
(10) Li, Z.; Mutlu, M.; Ozbay, E. Chiral metamaterials: from optical activity and negative refractive index to asymmetric transmission. *J. Opt.* **2013**, *15*, 023001.
(11) Wang, B.; Zhou, J.; Koschny, T.; Soukoulis, C. M. Nonplanar chiral metamaterials with negative index. *Appl. Phys. Lett.* **2009**, *94*, 151112.
(12) Schwanecke, A. S.; Fedotov, V. A.; Khardikov, V. V.; Prosvirnin, S. L.; Chen, Y.; Zheludev, N. I. Nanostructured metal film with asymmetric optical transmission. *Nano Lett.* **2008**, *8*, 2940−2943.
(13) Afshinmanesh, F.; White, J. S.; Cai, W.; Brongersma, M. L. Measurement of the polarization state of light using an integrated plasmonic polarimeter. *Nanophotonics* **2012**, *1*, 125−129.
(14) Rodríguez-Fortuño, F. J.; Marino, G.; Ginzburg, P.; O'Connor, D.; Martínez, A.; Wurtz, G. A.; Zayats, A. V. Near-field interference for the unidirectional excitation of electromagnetic guided modes. *Science* **2013**, *340*, 328−330.
(15) Lin, J.; Mueller, J. P. B.; Wang, Q.; Yuan, G.; Antoniou, N.; Yuan, X.-C.; Capasso, F. Polarization-controlled tunable directional coupling of surface plasmon polaritons. *Science* **2013**, *340*, 331−334.
(16) Huang, L.; Chen, X.; Bai, B.; Tan, Q.; Jin, G.; Zentgraf, T.; Zhang, S. Helicity dependent directional surface plasmon polariton excitation using a metasurface with interfacial phase discontinuity. *Light Sci. Appl.* **2013**, *2*, e70.

(17) Lee, S.-Y.; Lee, I.-M.; Park, J.; Oh, S.; Lee, W.; Kim, K.-Y.; Lee, B. Role of magnetic induction currents in nanoslit excitation of surface plasmon polaritons. *Phys. Rev. Lett.* **2012**, *108*, 213907.
(18) Righini, G. C.; Dumeige, Y.; Féron, P.; Ferrari, M.; Conti, G. N.; Ristic, D.; Soria, S. Whispering gallery mode microresonators: fundamentals and applications. *Riv. Nuovo Cim.* **2011**, *34*, 435−488.
(19) Cai, X.; Wang, J.; Strain, M. J.; Johnson-Morris, B.; Zhu, J.; Sorel, M.; O'Brien, J. L.; Thompson, M. G.; Yu, S. Integrated compact optical vortex beam emitters. *Science* **2012**, *338*, 363−366.
(20) Mie, G. Beiträge zur optik trüber medien, speziell kolloidaler metallösungen. *Ann. Phys.* **1908**, *330*, 377−445.
(21) Rodríguez-Fortuño, F. J.; Puerto, D.; Griol, A.; Bellieres, L.; Martí, J.; Martínez, A. Sorting linearly polarized photons with a single scatterer. *Opt. Lett.* **2014**, *39*, 1394.